Life Sciences 238 (2019) 116971

Contents lists available at ScienceDirect

Life Sciences

journal homepage: www.elsevier.com/locate/lifescie

Time-dependent alteration to the tight junction structure of distal intestinal epithelia in type 2 prediabetic mice

Ricardo Beltrame de Oliveira, Valquiria Aparecida Matheus, Leandro Pereira Canuto, Ariane De Sant'ana, Carla Beatriz Collares-Buzato*

Department of Biochemistry and Tissue Biology, Institute of Biology, University of Campinas (UNICAMP), Campinas, SP, Brazil

ARTICLE INFO

Keywords:
Tight junction
Intestinal epithelial barrier
Paracellular permeability
Type 2 diabetes mellitus
High-fat diet
Free fatty acids
Caco-2 cells

ABSTRACT

Aim: High-fat diet (HFD) intake has been associated with changes in intestinal microbiota composition, increased intestinal permeability, and onset of type 2 diabetes mellitus (T2DM). The aim of this work was twofold: 1) to investigate the structural and functional alterations of the tight junction (TJ)-mediated intestinal epithelial barrier of ileum and colon, that concentrate most of the microbiota, after exposure to a HFD for 15, 30 and 60 days, and 2) to assess the effect of *in vitro* exposure to free fatty acids (FFAs), one of the components of HFD, on paracellular barrier of colon-derived Caco-2 cells.

Methods/key findings: HFD exposure induced progressive metabolic changes in male mice that culminated in prediabetes after 60d. Morphological analysis of ileum and colon mucosa showed no signs of epithelial rupture or local inflammation but changes in the junctional content/distribution and/or cellular content of TJ-associated proteins (claudins-1, -2, -3, and occludin) in intestinal epithelia were seen mainly after a prediabetes state has been established. This impairment in TJ structure was not associated with significant changes in intestinal permeability to FITC-dextran. Exposure of Caco-2 monolayers to palmitic or linoleic acids seems to induce a reinforcement of TJ structure while treatment with oleic acid had a more diverse effect on TJ protein distribution.

Significance: TJ structure in distal intestinal epithelia can be specifically impaired by HFD intake at early stage of T2DM, but not by FFAs *in vitro*. Since the TJ change in ileum/colon was marginal, probably it does not contribute to the disease onset.

1. Introduction

One of the major risk factors for the development of type 2 diabetes (T2DM) is obesity, which in turn is a result of intake of high fat and high carbohydrate diet associated with a sedentary lifestyle. T2DM is a metabolic disease highly prevalent worldwide and, although its pathogenesis has not yet been fully elucidated, it is known that the interaction between genetic predisposition and environmental factors (such as obesity itself) are crucial for the disease onset [1,2]. T2DM is initially characterized by moderate hyperglycemia and insulin resistance associated with compensatory hyperinsulinemia and low-grade systemic inflammation [2,3]. As the disease progresses, the pancreatic compensatory response to insulin resistance is no longer efficient and exogenous insulin is needed at later stages to regulate glycemic levels [1,4–6].

The increase in serum lipids and free fatty acids (FFA) associated with high-fat-feeding have been proposed to be key factors leading to an increased tissue resistance to insulin and β-cell dysfunction that culminates in T2DM [7,8]. It has been suggested that a lipid-rich-diet intake may also lead to a change in the gut microbiota, which is associated with an impaired intestinal barrier, endotoxemia and low-grade inflammation that together may play a role in the development of T2DM [9–11]. The current hypothesis, which attempts to explain the involvement of the intestinal microbiota in the pathogenesis of diabetes, suggests that the change in the composition and diversity of this microbiota, due at least in part to a low-fiber and high-fat diet, is associated with impairment of the intestinal barrier. This, in turn, would lead to the systemic entry of bacteria and their products, as well as food allergens, resulting in hypersensitivity of the immune system in the case of type 1 diabetes, or a low-grade endotoxemia and systemic inflammation, contributing to the triggering or aggravation of the peripheral resistance to insulin in type 2 diabetes [10,12–17]. Therefore,

* Corresponding author. Department of Biochemistry and Tissue Biology, Institute of Biology, University of Campinas – UNICAMP, CEP 13083-970, Campinas, São Paulo, Brazil.
E-mail address: collares@unicamp.br (C.B. Collares-Buzato).

https://doi.org/10.1016/j.lfs.2019.116971
Received 13 July 2019; Received in revised form 13 October 2019; Accepted 14 October 2019
Available online 18 October 2019
0024-3205/

according to this hypothesis, the intestinal barrier would constitute a central factor in the relationship between microbiota and metabolic alterations associated with diabetes.

The intestinal barrier relies on a set of different elements, such as the intestinal epithelium itself in conjunction with antimicrobial peptides, antibodies, and mucus secreted by mucosa-associated cells. This barrier controls the intestinal bacterial growth and limits intestinal microorganism translocation and/or the absorption of harmful agents present in the intestine milieu [18–22]. The intestinal paracellular barrier is regulated by the tight junctions (TJ) that bind intestinal epithelial cells together [20,23–25]. The TJ is a plasma membrane specialization constituted by integral transmembrane proteins (such as claudins and occludin), which interact laterally with each other and to intracellular proteins (such as ZO-1, -2, -3, cingulin, 7H6 antigen, simplekin, etc) that, in turn, are anchored to the cytoskeletal actin microfilaments. Besides taking part in cell adhesion and cell polarity, the TJ acts as a selective barrier that restrains the free passage of ions, molecules, and cells through the paracellular space (between cells), thus forming an important element of the intestinal barrier [22,24,26,27].

Studies on the relationship between diet, intestinal barrier and diabetes have mainly focused on the role of the modified intestinal microbiota and its metabolites on the metabolic changes and immune response of the organism affected by this metabolic dysfunction and possible reversion of the condition after treatment with pre-, pro- and post-biotics [17,28–30]. Few works have addressed the role of TJ-mediated epithelial barrier in this process, even so this was marginally done [10,12,15]. In a pioneering work, Cani et al. [10] described an increased intestinal permeability associated with the reduction of ZO-1 and occludin gene expression in intestinal homogenates of C57 mice fed a hyperlipidic diet, that also displayed metabolic alterations and endotoxemia. Corroborating the idea of a role of the intestinal paracellular barrier in the obesity-related T2DM pathogenesis, we have recently shown that *in vitro* exposure to intestine luminal content isolated from high-fat diet-fed prediabetic mice induced a significant increase in paracellular permeability in Caco-2 and MDCK epithelial cell lines, which was accompanied by a significant decrease in junctional content of barrier-forming claudins, occludin, and ZO-1, indicative of disruption of the TJ barrier [31].

Despite all evidence of the relationship between impaired intestinal barrier and diabetes, the mechanisms underlying the phenomenon are still unclear. Does the increased intestinal permeability observed in patients and diabetic animals [10,13,32–35] involve specific regulation of the TJ in the intestinal epithelium or this would be result from lesion of the epithelium as a consequence of a local inflammatory process? What is the temporal correspondence between the onset of T2DM-associated metabolic alterations and the TJ-mediated intestinal barrier disruption? Which intestinal luminal component would be responsible for the impaired intestinal barrier observed in diabetic patients [13,32,35], in animal models of T2DM [10,30,33,34] and *in vitro* conditions [31]? In order to address some of these questions, the aim of the present work was two-fold: 1) to investigate the structure and function of TJ-mediated intestinal epithelial barrier in parallel to the metabolic alterations in our animal model of type 2 prediabetes [5,30,36], by employing C57 mice fed a high-fat diet for different periods of time (i.e. 15d, 30d, and 60d); and 2) to study the effect of FFA, one the main components of a high-fat diet (particularly palmitic acid, oleic acid, and linoleic acid) [37–39], on the epithelial paracellular barrier function *in vitro*. For the *in vivo* study, we evaluated the structure and function of the TJ-mediated intestinal barrier in the ileum and colon, since these segments are representative of the small and large intestine, respectively, and concentrate most of the intestinal microbiota [16,40,41]. For the *in vitro* experiments, we have used a human colon adenocarcinoma-derived epithelial cell line, the Caco-2 cells, that share several features of enterocytes [42,43].

2. Material and methods

2.1. Animals and diet

Male C57BL/6JUnib mice, aged between 16 to 20 weeks, were obtained from the Multidisciplinary Center for Biological Investigation on Laboratory Animal Science (CEMIB) of the University of Campinas (UNICAMP, Brazil) and kept at 22–25 °C on a 12 h light/dark cycle. The animals were fed a standard chow diet (content in 100 g: 4.5 g lipids, 53 g carbohydrates and 23 g proteins) (Nuvital CR1, Colombo, Paraná, Brazil) (Control, Ctrl) or a high-fat diet (HFD) (content in 100 g: 21 g lipids, 50 g carbohydrates and 20 g proteins) ad libitum for 15, 30 or 60 days. All experimental protocols were approved by the Ethics Committee on Animal Use (CEUA) of UNICAMP under protocol #3040–1.

2.2. Metabolic evaluation

Mice from each experimental group (control and HFD) exposed to their respective diet for one of the time period tested (15, 30 or 60d) were independently evaluated regarding their metabolic state. Body weight, fasting and fed glycemia, and insulin tolerance test (ITT) were evaluated after the experimental period. For ITT, fed mice had their initial blood glucose measured (using Accu-Chek Advantage II glucometer – Roche – Switzerland) before intraperitoneal insulin injection (t = 0) (0.5 U/kg – Biobrás – MG – Brazil) and at 10, 15, 30, and 60 min thereafter. The plasma biochemical analysis, i.e. fast plasma insulin (Kit Rat/Mouse Insulin ELISA Kit - Merck EZRMI-13K), serum cholesterol (Colestatt Enzymatic AA - Weiner Lab, REF 1220114), serum triglycerides (TG Color - Weiner Lab, REF 1780105), serum HDL (HDL Cholesterol - Weiner Lab, REF 1220103) and serum LDL cholesterol (Weiner Lab, REF 1220104) were carried out using commercial kits and following the manufacturer's instructions. Body weight and blood samples were collected between 9:00 and 11:00 a.m.

2.3. Histology of the intestinal segments

Distal ileum and proximal colon fragments from all experimental groups were fixed for 18 h in 4% paraformaldehyde solution (in 0.1 M Phosphate buffered saline (PBS), pH 7.4), then washed 4 times in distilled water and kept in 70% alcohol in the refrigerator for up to 3 days. Subsequently, fragments were dehydrated in a series of ethanol solution of increasing concentrations (80%, 95%, 100% I, 100 II and 100% III for 30 min each), followed by diaphanization (1:1 ethanol/xylene, xylene I and xylene II for 15 min each), paraffin embedding (1:1 xylene/paraffin 30 min and paraffin for 2 h) and finally paraffin inclusion (Histosec-Merck). Fragments were then semi-serially sectioned (5 μm-thick slice), followed by a standard protocol for hematoxylin and eosin staining. The sections were photographed by a light microscope (Olympus - BX51) coupled with a digital camera (Olympus Q-Color 3). Images from intestinal histological slices were obtained with an objective of 10x (villus) or 40x (crypt) for posterior morphometric analysis [44]. Villus length/width or crypt depth/width were measured using the straight-line tool of the ImageJ software (https://imagej.nih.gov/ij/) and expressed as μm. The measurement of the villi was considered from its apex to its base, while crypt was measured from its opening to its base. The villus width was measured near the base of the villus. At least 10 villi and 10 crypts per image were analyzed from at least 2 histological slices per animal (number of animals/group: 5–6). The mean values of each measured parameter for each portion of the intestine in each animal were evaluated and entered as raw data on the database.

2.4. Immunofluorescence for tight junction proteins

Immunofluorescence was performed to assess whether HFD induces

changes in the distribution of TJ-associated proteins (claudins-1, -2, and-3, and occludin). Therefore, intestinal fragments (ileum and colon) were collected, washed in 0.05 M PBS (pH7.4), and frozen with Tissue-Tek® medium at −65 °C in n-hexane. Subsequently, the cryosections were fixed in −20 °C acetone for 3 min and stored at −80 °C until immunofluorescence staining. Slides were washed in PBS, permeabilized with 0.1% Triton (TPBS, 0.1% Tween 20 in 0.05 M PBS plus 5% albumin), and incubated with primary antibody (in PBS plus 3% albumin; Rabbit anti-Claudin-1, dilution 1:30 (Abcam ab15098); Rabbit anti-Claudin-2, dilution 1:30 (Abcam 53032); Rabbit anti-Claudin-3, dilution 1:50 (Invitrogen 34–1700); Rabbit anti-Occludin, dilution 1:40 (Abcam ab31721)) for 2 h at room temperature (RT). Cryosections were then washed with PBS, incubated for 2 h with secondary antibody conjugated with FITC (Goat anti-Rabbit-FITC, dilution 1:75 (Sigma F0382) in PBS plus 1% albumin + DAPI, dilution 1: 1000 (Sigma D9542)), washed again in PBS, mounted with Vectashield (Vector Laboratories, Inc., Burlingame, CA) or ProLong® Gold Antifade Mountant (Invitrogen P36930), and finally photographed using a fluorescence microscope (Observer.Z1; Zeiss - Axio Cam MRC, Hamburg, Germany, or Leica DM5500 B). To evaluate fluorescence intensity and compare experimental groups, intestine sections from both groups (control and HFD groups) were processed for immunofluorescence at the same time and analyzed at the same observation session, using identical microscope parameters for image capture. The fluorescence degree was evaluated using the ImageJ software, in which 60 points per image were randomly selected from 5 random areas of each cryosection photographed (2–3 sections/animal, 3–11 animals/group, from at least three independent experiments). Each point was placed exclusively at the intercellular contact in the intestinal epithelium (adding up to 833–2770 points sampled per experimental group). Fluorescence degree data, which represents the junctional content of a given TJ protein, were expressed as an arbitrary unit of fluorescence.

2.5. Western blotting for tight junction-associated proteins

Ileum and colon fragments were washed with PBS, the epithelium scraped with a surgical scalpel and homogenized in an anti-protease cocktail (composition: 10 mM imidazole pH 7.4; 4 mM EDTA; 1 mM EGTA; 200 μM DTT; 0.5 μg/mL pepstatin A; 200 KIU/mL aprotinin; 200 μM PMSF; 2.5 μg/mL leupeptin e 30 μg/mL trypsin inhibitor). An amount of 40 μg of protein from each sample was incubated for 1 h at 37 °C in Laemmli sample buffer (30% of volume), separated by electrophoresis in 12% polyacrylamide gels, and then transferred to a nitrocellulose membrane (Bio-Rad). Subsequently, membranes were blocked overnight at 4 °C with TTBS (0.1% Tween 20 in 0.05 M Tris-saline Buffer plus 5% dry skimmed milk) and then incubated at RT for 2 h with a primary antibody (Rabbit anti-Claudin-1, dilution 1:300 (Abcam ab15098), Rabbit anti-Claudin-2, dilution 1:200–1:500 (Abcam ab53032), Rabbit anti-Claudin-3, dilution 1:500 (Invitrogen 34–1700), Rabbit anti-Occludin, dilution 1:500 (Abcam ab31721), Rabbit anti-Beta-actin, dilution 1:500–1:700 (Cell Signaling 4970S)) diluted in TTBS plus 3% dry skimmed milk. Membranes were rinsed with TTBS and incubated with HRP-conjugated specific secondary antibody (Goat anti-rabbit HRP, dilution 1:500–1:1000 (Sigma A4914)) diluted in TTBS plus 1% skimmed milk powder for 2 h at RT. Band signal was developed by an enhanced chemiluminescence kit (SuperSignal West Pico Chemiluminescent Substrate, Thermo Fisher Scientific), acquired in a G:box system (Syngene - UK), and quantified by optical densitometry (Image J). Finally, membranes were reprobed with anti-beta-actin antibody (internal control) and optical densitometry values were expressed as the ratio of the TJ protein/beta-actin.

2.6. Intestinal permeability to FITC-dextran

2.6.1. Gavage

The intestinal paracellular permeability was assessed employing the fluorescein isothiocyanate (FITC)–dextran 4000 (Sigma) as a permeability marker. At the end of the experimental period, mice were fasted for 6 h before receiving the FITC- dextran (Sigma 46944) solution via gavage, (600 mg/kg in 7 ml/kg in sterile saline) [10]. After 2 h, animals were euthanized, the blood sample was collected from the cervical vessels and centrifuged at 10,644 × *g*, at 4 °C, for 10 min. FITC-Dextran concentration was measured in the plasma with a Fluorskan Ascent microplate reader (Thermo Scientific), at wavelengths of 458 nm (excitation) and 535 nm (emission). As a positive control, a different experimental group developed colitis by ingestion of dextran sodium sulfate (3% w/v - Sigma 42867) mixed with drinking water for 7 days [45]. The FITC-dextran plasma concentration was expressed as absolute Absorbance value after subtracting the blank plasma value (obtained from tail vein blood of mice that not received the marker).

2.6.2. Intestinal sacs

A surgical procedure was performed to assess the paracellular permeability in the two intestine segments, ileum and colon, separately [46]. Mice were fasted for 12 h, anesthetized with ketamine/xylazine (80 + 10 mg/kg) and had their blood sampled from the tail vein for blank plasma measurement. The intestine was exposed through a laparotomy incision, an intestinal sac (2 cm in length) was created with a suture-loop at each end in the ileum or proximal colon and 50 μL FITC-dextran solution (100 mg/mL sterile saline) were injected with BD Ultra-Fine™ needle into the intestine sac lumen. Subsequently, the intestine was placed back into the abdominal cavity, the animal was sutured and kept under anesthesia until euthanasia. After 1 h, the animals were decapitated, blood was collected from the cervical vessels in heparinized microtubes and centrifuged (10,644 × *g*/10 min at 4 °C) to obtain the plasma. The samples were diluted 1:4 in sterile saline and plasma fluorescence measured on the Synergy H1 (Biotek) microplate reader at wavelengths of 458 nm (excitation) and 535 nm (emission). As described above, the FITC-dextran plasma concentration was expressed as absolute Absorbance value after subtracting the blank plasma value.

2.7. Cell culture and in vitro paracellular barrier analysis

Caco-2 cells were cultured in high glucose DMEM medium supplemented with 10% FBS, 2% non-essential amino acids, 1% L-glutamine and 60 mg/L gentamicin (Cultilab – Campinas, Brazil) at 37 °C in a 5% CO_2 humidified incubator (Incusafe Sanyo MCO-17A, Sanyo Electric Ltd., Japan). Cells were seeded, at the density of $1.5x10^4$ cells/cm^2, on 12 mm diameter cell culture inserts (MILLICELL), coated with collagen extracted from Wistar rats tails [47]. When fully confluent (10–11 days after seeding), monolayers were exposed at both sides (apical + basal) to Krebs solution (composition in mM: NaCl 115, KCl 5, $MgCl_2$ 1, $CaCl_2$ 1.24, $NaHCO_3$ 1, HEPES 15; pH = 7.4 equilibrated with CO_2 5%), containing or not 200 μM or 400 μM palmitic, oleic or linoleic acid (Sigma) for 24 h. The concentrations and time of exposure to these fatty acids have been chosen since they are parameters below to those with known cytotoxic action [43,48,49], but are within the plasma concentrations reported for obese and/or diabetic individuals [50–52].

Transepithelial electrical resistance (R_T) across Caco-2 monolayer was evaluated for 24 h with a voltmeter (EVOM, World Precision Instruments, UK). The final R_T value (Ω·cm^2) was calculated by subtracting the cell culture insert membrane resistance (without cells) and multiplied by the membrane area (1.13 cm^2) [31]. For the measurement of the transepithelial flux (F_T), we have used the FITC-dextran (MW 4000 Da) and a small-sized molecule, the phenol red (MW 354 Da - Sigma), as paracellular markers [31]. Monolayers grown on 30 mm diameter inserts were exposed at both apical and basal surfaces to different concentrations of fatty acids, and phenol red (100 μM) or FITC-dextran (100 μM) was added only in the basal solution. After the incubation period, a volume of 0.2 mL of each apical and basal solution was collected in triplicate. The absorbance reading of phenol red samples was performed in a microplate reader (Power Wave, Biotek

Instruments, U.S.A) using a wavelength of 492 nm. FITC-Dextran samples were read at wavelengths of 458 nm (excitation) and 535 nm (emission) using the Fluorskan Ascent microplate reader (Thermo Scientific). For the calculation of F_T, the absorbance of the apical solution was expressed as a percentage in relation to the sum of the absorbance of the basal plus the apical solution (considered as 100% of the marker concentration), according to the formula below:

$$F_T = Absa \times 100 / (Absa + Absb)$$

where Absa represents the absorbance of the apical solution and Absb is the absorbance of the basal solution.

The immunofluorescence reaction for some junctional proteins (namely claudin-1, occludin, and ZO-1) was performed in Caco-2 monolayers kept in methanol at −20 °C. Monolayers were washed with PBS, incubated with 3% fetal bovine serum in PBS for 30 min and subsequently, we followed the same steps and used the same primary antibodies and respective dilutions described above for immunofluorescence in cryosections. As for Western Blot, Caco-2 monolayers were scraped from cell culture inserts and processed as described above for intestine homogenates, except that an amount of only 20 µg of proteins was loaded into the polyacrylamide gel, using the same primary antibodies and dilutions described above for immunoblotting.

2.8. Statistical analysis

Statistical analysis was performed using the GraphPad Prism 5 software (GraphPad Software, La Jolla, Ca, USA). Results were expressed as the mean ± standard error of the mean (SEM). Statistical differences between the two groups (control and HFD) were assessed by Student's t-test (two-tailed). For multiple statistical comparisons among the groups in the *in vitro* experiments, we have used the One-way analysis of variance (ANOVA) followed by the Bonferroni's post-test to compare pairs of data. The statistical significance level was set at $P < 0.05$, except for the immunofluorescence data where the limit was $P < 0.0001$.

3. Results

Body weight, fasting and postprandial glycemia, fasting insulinemia, peripheral insulin resistance test (ITT) and lipid profile were assessed to characterize the metabolic state of the animals fed a high-fat (HFD) or chow diet (Ctrl) for 15d, 30d and 60d.

As shown in Fig. 1, after 15d, HFD induced a significant increase ($P < 0.01$) in body weight (Fig. 1a) and post-prandial glycemia (Fig. 1c) in relation to Ctrl group. At 30d, in addition to weight gain ($P < 0.001$) and postprandial hyperglycemia ($P < 0.001$), HFD induced an increase in fasting glucose (Fig. 1b) ($P < 0.05$). At the end of the treatment (60d), HFD-fed mice became obese ($P < 0.001$) and displayed fasting ($P < 0.001$) and postprandial hyperglycemia ($P < 0.001$), as well as fasting hyperinsulinemia (Fig. 1d) ($P < 0.001$) when compared to the Ctrl group. Insulin tolerance test (ITT, Fig. 1e) showed no significant changes in the response to this hormone in mice fed a HFD for 15d or 30d in relation to Ctrl animals, however, after 60d they developed insulin resistance ($P < 0.05$) as shown by the analysis of the incremental area under the ITT curve (Fig. 1e). Moreover, the lipid profile revealed that, in relation to the Ctrl group, HFD-fed mice showed increased serum cholesterol from 15d of treatment (Fig. 1f) ($P < 0.001$), total triglycerides from 30d (Fig. 1g) ($P < 0.05$), and LDL levels at 60d (Fig. 1h) ($P < 0.05$) with no significant alteration in HDL concentration (Fig. 1i).

Histological analysis of ileum and colon did not show apparent lesions in the intestinal lining epithelium of mice fed a HFD in relation to the Ctrl group, during all periods studied (Fig. 2). Also, no structural changes were observed in the lamina propria and submucosa layers nor an abnormal or increased presence of lymphocytic infiltrates in treated mice, which would indicate a local inflammatory process.

In order to analyze the HFD effect upon the TJ structure in the intestinal epithelium, the cellular distribution and content of some TJ proteins (i.e. claudins-1, -2 and -3, and occludin) were evaluated by immunofluorescence in intestine cryosections and by immunoblotting in intestinal epithelium homogenates, respectively (Figs. 3–6). Immunofluorescence analysis of the Cld-1 junctional content in the ileum and colon regions (Fig. 3e, k, q) revealed a significant decrease ($P < 0.0001$) in both segments in mice exposed to HFD for 60d, in comparison to the Ctrl group. Regarding the analysis of the total cellular content of Cld-1 in ileal and colonic epithelium homogenates by immunoblotting, no significant difference was observed between HFD and Ctrl groups in any of the studied periods (Fig. 3f, l, r). The HFD intake induced a significant decrease in the junctional content of Cld-2 ($P < 0.0001$) in the epithelial cell of colon at 15d and ileum at 60d, and an increase of this protein in the colon epithelium at 60d (Fig. 4e, k, q). In addition, the total cellular content quantification of Cld-2 showed

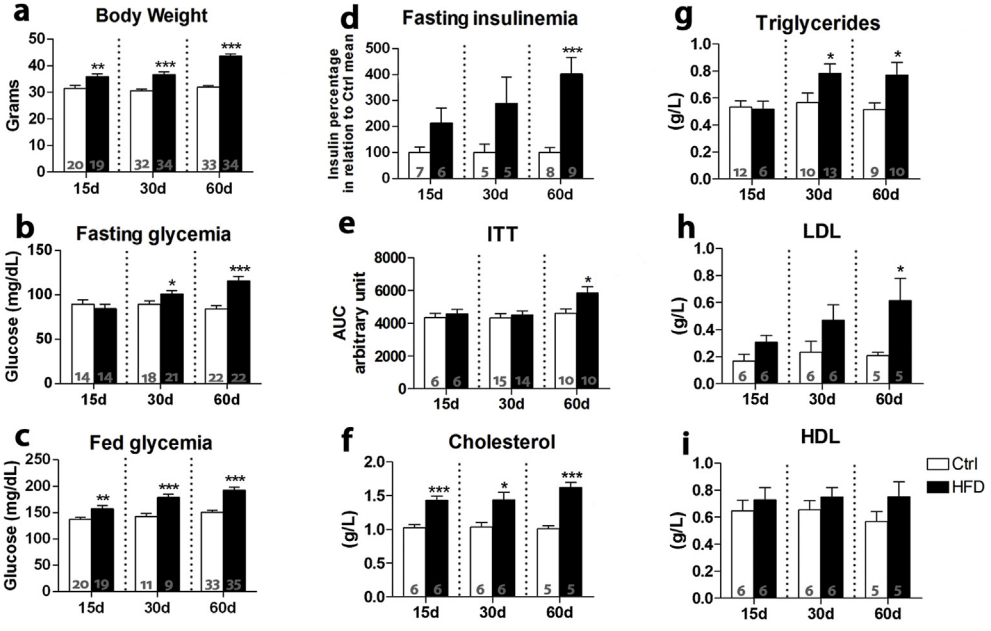

Fig. 1. Metabolic parameters in mice fed a standard (Ctrl) or high-fat diet (HFD) for 15d, 30d and 60d. HFD induced a significant weight gain (a), hyperglycemia in the fed state (c) and cholesterol (f) from 15d. After 30d, HFD-fed mice also displayed fast hyperglycemia (b) and high triglycerides plasma level (g). In addition to all these alterations, the 60d-HFD-fed mice developed insulin resistance as demonstrated by the incremental area under the curve (AUC) (e) and fast hyperinsulinemia (d) as well as high levels of LDL (h). Results are expressed as mean ± SEM from *n* samples shown in the graph bar. *$P < 0.05$, **$P < 0.01$ and ***$P < 0.001$ as compared to its Ctrl group (Student t-test).

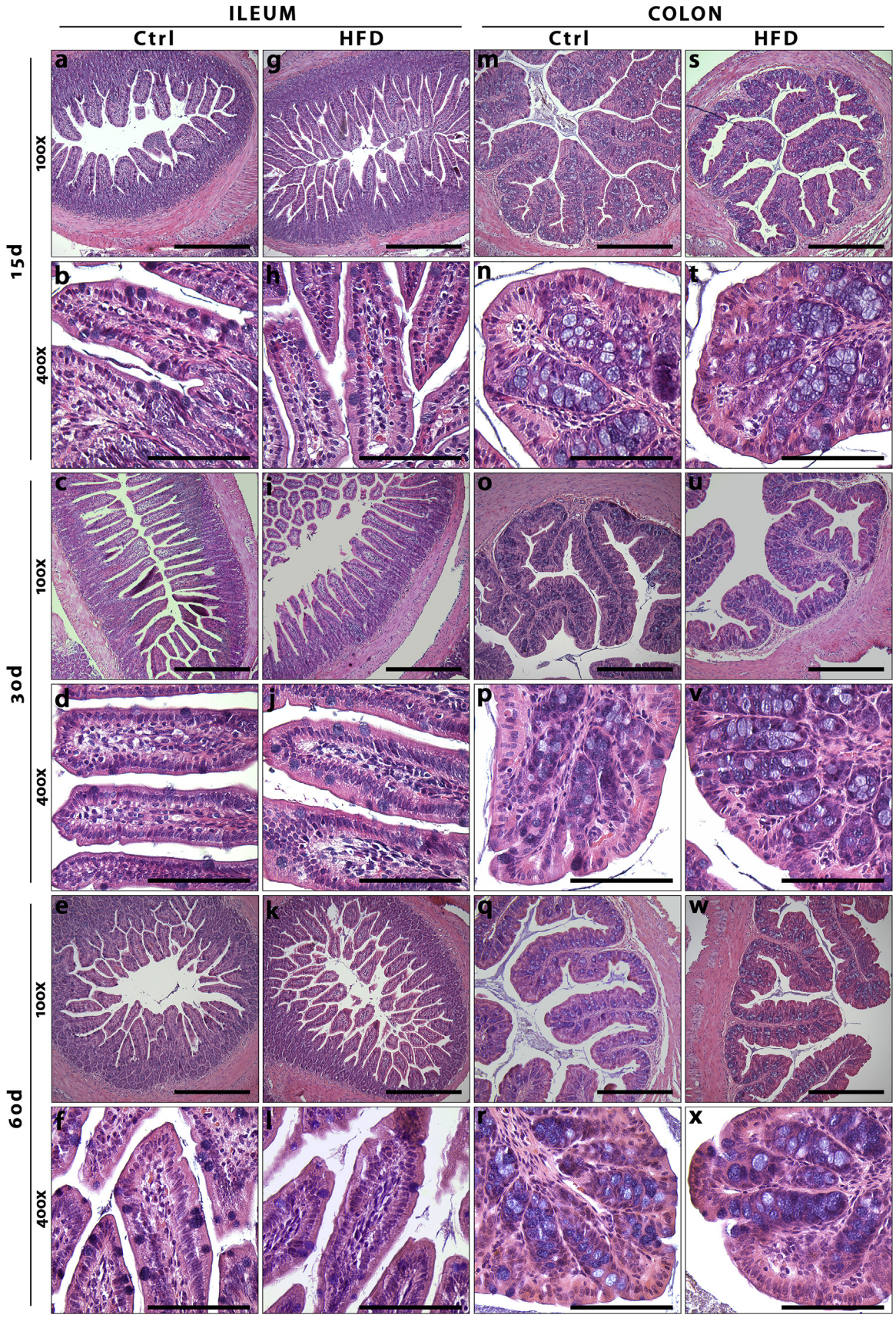

Fig. 2. Histological analysis of the ileum and colon of mice fed a standard (Ctrl) or a high-fat diet (HFD) for 15d, 30d and 60d. Morphological analysis of these intestinal segments was performed on histological sections stained with Hematoxylin and Eosin. In all periods studied, no marked morphological alteration in the intestinal epithelium was observed in ileum and colon segments (400x images) from animals treated with HFD in comparison with the Ctrl ones. Also, there were no changes suggestive of inflammation (inflammatory cell infiltration) in the lamina propria and submucosa, in the experimental groups (100x and 400x images). Bar: 400 μm (100x images) and 100 μm (400x images).

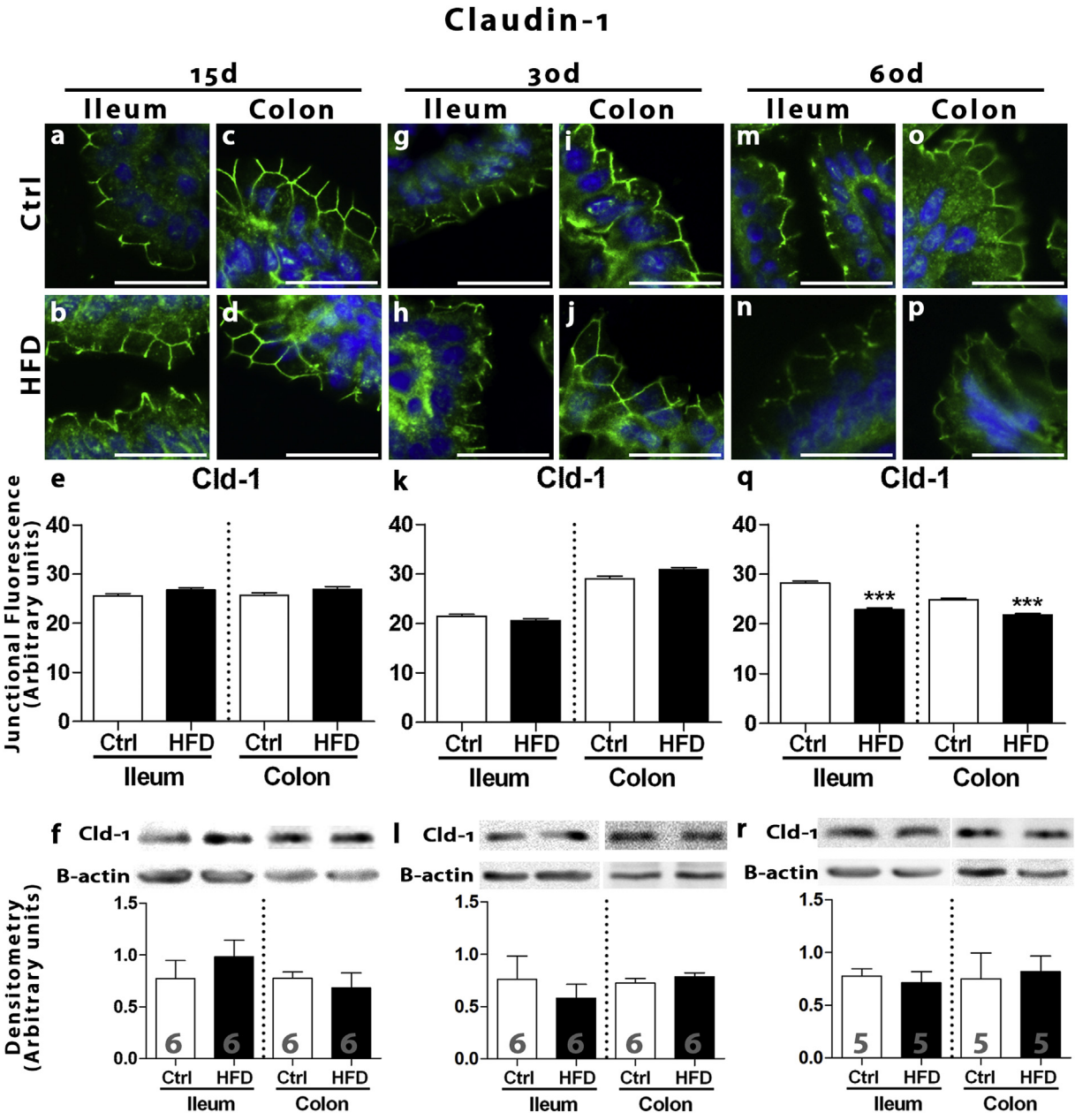

Fig. 3. Cellular distribution and content of Claudin-1 in the epithelium of ileum and colon from mice fed a standard (Ctrl) or high-fat diet (HFD) for 15d, 30d and 60d. Images a-d, g-j, m-p show the junctional labeling of claudin-1 evidenced by immunofluorescence (FITC in green, DAPI-blue labeling of the nucleus) in cryosections of ileum and colon of mice treated with HFD for different periods. The images of Ctrl and HFD groups are representative, obtained from the same immunofluorescence and microscopic session. At 15 d and 30 d, HFD did not induce a significant change in the Cld-1 junctional labeling (e, k), but after 60d of treatment, the animals showed a significant reduction of this protein at the intercellular region of the epithelium of ileum and colon (q). The immunoblotting did not show significant alteration in the total cellular content of Cld-1 in homogenates of the epithelium of the ileum and colon between the groups during the time periods studied (f, l, r). Bar, 25 μm. The number inside the bars shows the number of animals for each group. The values represent the mean ± SEM. ***P < 0.0001 compared to its Ctrl group (Student t-test). (For interpretation of the references to colour in this figure legend, the reader is referred to the Web version of this article.)

only a significant decrease in the ileal epithelium of animals fed HFD for 60d ($P < 0.05$; Fig. 4f, l, r). In relation to Cld-3 junctional content, a significant decrease of this TJ protein in the ileal epithelium ($P < 0.0001$) was observed after 30 and 60d of HFD treatment (Fig. 4e, k, q). Similarly, to Cld-1, the total cellular content of Cld-3 remained unchanged between the intestinal segments, groups and time periods studied (Fig. 5f, l, r). Occludin immunofluorescence revealed a significant decrease in this protein content at the intercellular contact in the ileal epithelium at 15 d and in the colon at 30 d and 60 d ($P < 0.0001$) in mice treated with HFD (Fig. 6 e, k, q) as compared to the Ctrl groups. These alterations, however, were not accompanied of significant changes in the total protein content of occludin in homogenates from the intestinal epithelium of HFD mice in comparison with the Ctrl group (Fig. 6 f, l, r).

The function of the TJ-mediated intestinal epithelial barrier was assessed using the paracellular FITC-dextran marker given to the animal by gavage or injected within intestine sacs *in situ*. The gavage method showed an increase of 174% ($P < 0.001$; Fig. 7 a) of the presence of the probe in the plasma of mice that received DSS (an animal model of colitis) in comparison with its control group. As for mice exposed to HFD for 15d, 30d or 60d, however, there were no significant changes in the intestinal permeability when compared to the Ctrl group (Fig. 7 a).

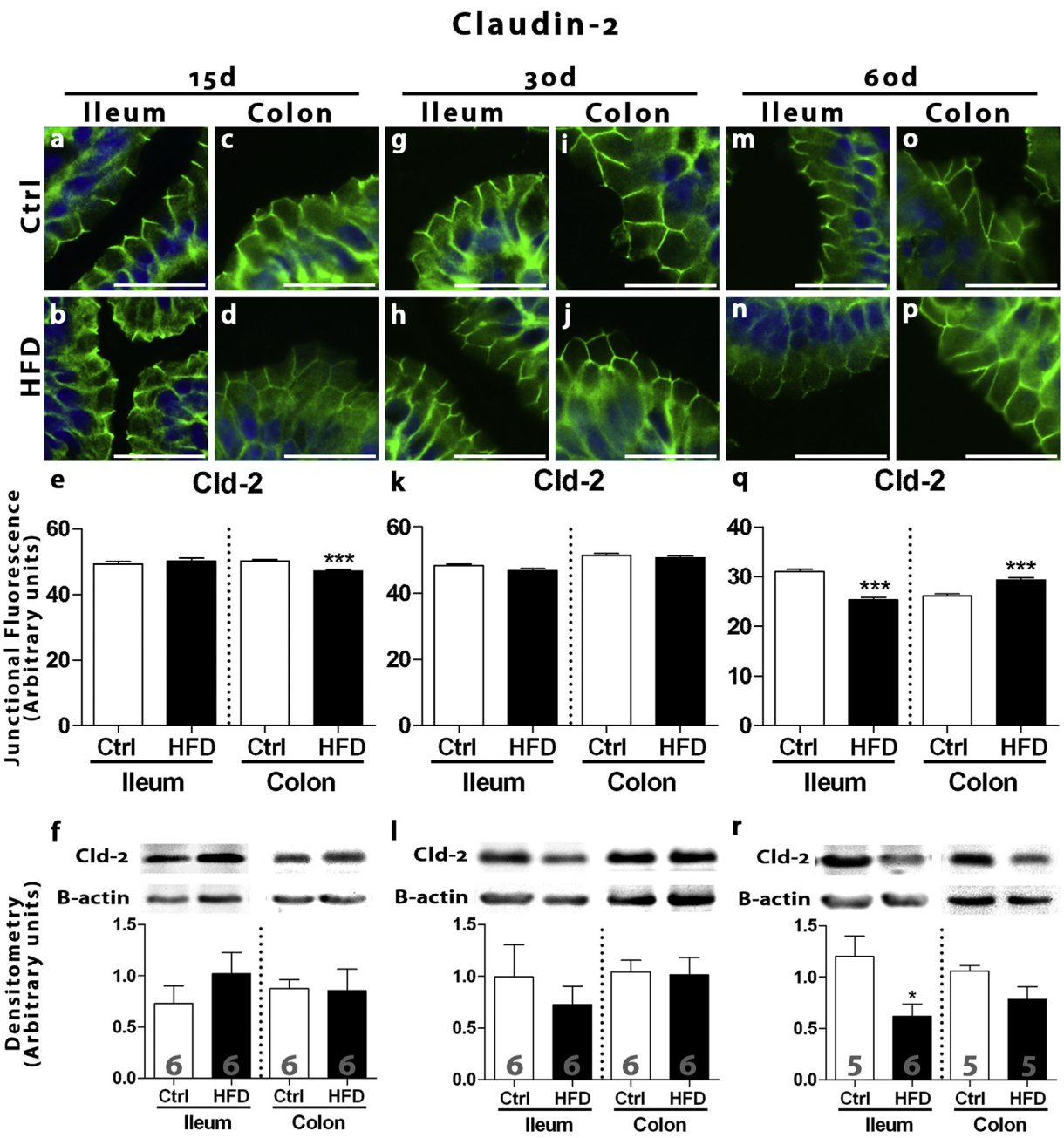

Fig. 4. Cellular distribution and content of Claudin-2 in the epithelium of ileum and colon from mice fed a standard (Ctrl) or high-fat diet (HFD) for 15d, 30d and 60d. Images a-d, g-j, m-p show the junctional labeling of claudin-2 evidenced by immunofluorescence (FITC in green, DAPI-blue labeling of the nucleus) in cryosections of ileum and colon of mice treated with HFD for different periods. The images of Ctrl and HFD groups are representative, obtained from the same immunofluorescence and microscopic session. HFD intake induced significant changes in the junctional content in the epithelium of the colon at 15 d (e) and of the ileum and colon after 60 d (q). The immunoblotting shows no significant alterations in the total cellular content of claudin-2 in intestinal epithelia of HFD-fed animals during the 15d (f) and 30d (1) periods, but a significant reduction in the epithelial content of this protein was observed in the ileum of 60d-HFD treated mice (r). Bar, 25 μm. The number inside the bars shows the number of animals for each group. The values represent the mean ± SEM. ***P < 0.0001 compared to its Ctrl group (Student t-test). (For interpretation of the references to colour in this figure legend, the reader is referred to the Web version of this article.)

In agreement with these results, the analysis of the permeability in isolated segments of the intestine (intestine sacs) also showed no significant changes in the ileum and colon permeabilities in 30d or 60d HFD-fed mice as compared to their controls (Fig. 7b and c). It should be mentioned though that, with both methods, a tendency of a decrease in the intestinal permeability to the FITC-dextran was observed in the HFD-fed mice (particularly regarding the ileum permeability) (Fig. 7 b). This observation could indicate a slight increase in tightness of the intestinal barrier after HFD intake (contrasting with our data on TJ proteins that suggest TJ disruption) or, alternatively, would be a result of a decrease of the intestinal absorption surface area. To test the latter, we performed a morphometric analysis to measure several parameters (i.e. villus/crypt width and length, in micrometers) of the intestinal mucosa of the different experimental groups. In ileum, we observed a significant decrease in villus length (60d-HFD group 222.80 ± 12.67 μm (n = 5 mice; 51 villi) *vs* Ctrl 259.40 ± 8.31 μm (n = 5 mice; 67 villi); *P < 0.05), crypt depth (60d-HFD group 48.66 ± 1.99 μm (n = 5 mice; 55 crypts) *vs* Ctrl 59.50 ± 3.39 (n = 5 mice; 61 crypts); *P < 0.03) and crypt width (60d-HFD group 23.75 ± 1.09 (n = 5 mice; 55 crypts) *vs* Ctrl 29.82 ± 1.67 (n = 5

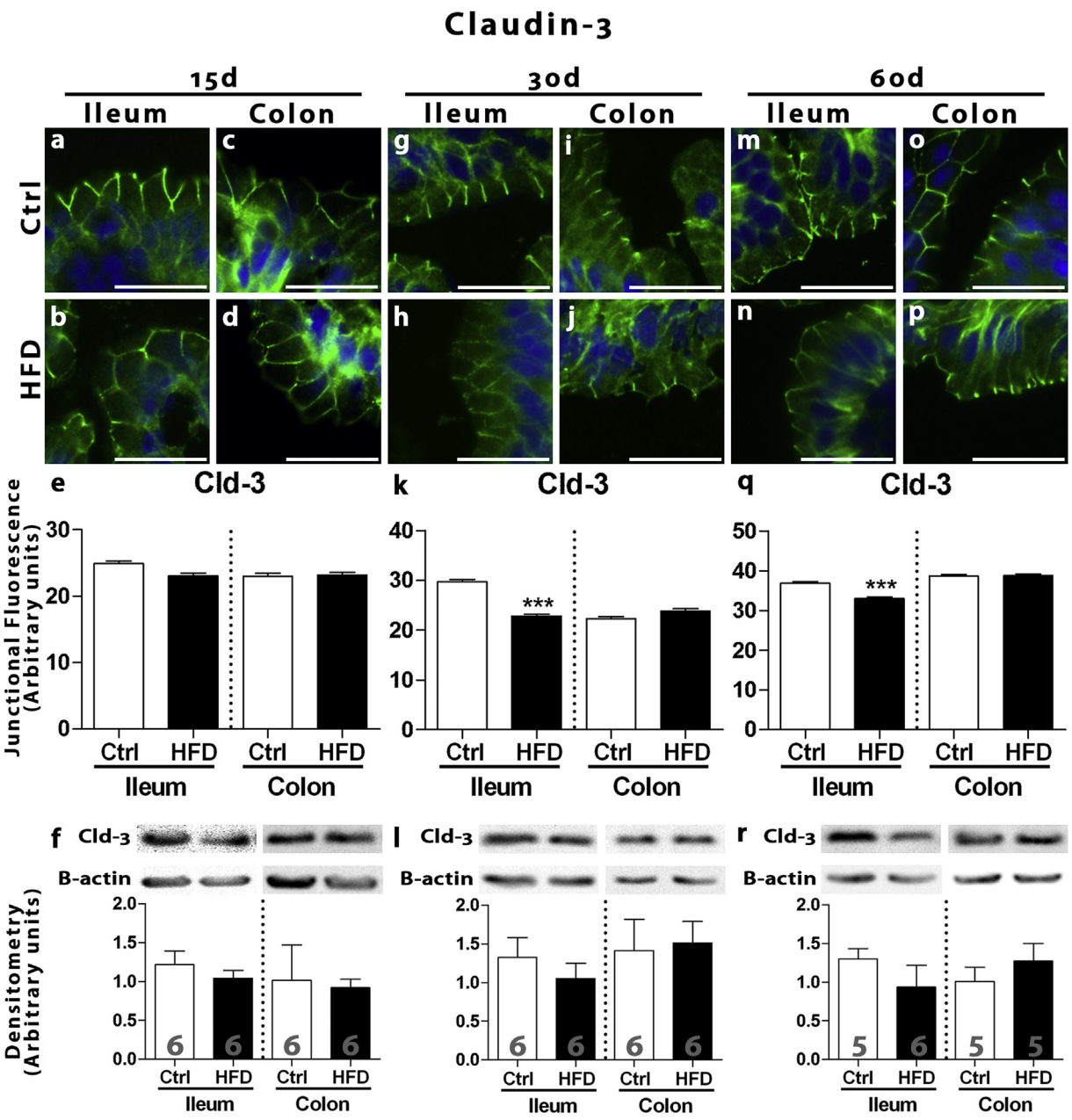

Fig. 5. Cellular distribution and content of Claudin-3 in the epithelium of ileum and colon from mice fed a standard (Ctrl) or high-fat diet (HFD) for 15d, 30d and 60d. Images a-d, g-j, m-p show the junctional labeling of claudin-3 evidenced by immunofluorescence (FITC in green, DAPI-blue labeling of the nucleus) in cryosections of ileum and colon of mice treated with HFD for different periods. The images of Ctrl and HFD groups are representative, obtained from the same immunofluorescence and microscopic session. HFD induced no significant change in junctional labeling of intestinal epithelia at 15 d (e), but resulted in a significant reduction in the intercellular labeling of Cld-3 in the epithelium of ileum, but not in the colon, after 30d and 60d of treatment in relation to the Ctrl group (k, q). The immunoblotting showed no significant change in the total cellular content of Cld-3 in homogenates of the epithelium of the ileum and colon between the groups during the time periods studied (f, l, r). Bar, 25 μm. The number inside the bars shows the number of animals for each group. The values represent the mean ± SEM. ***P < 0.0001 compared to its Ctrl group (Student t-test). (For interpretation of the references to colour in this figure legend, the reader is referred to the Web version of this article.)

mice; 61 crypts); *P < 0.02) but no change in villus width (60d-HFD group 54.88 ± 2.57 (n = 5 mice; 51 villi) *vs* Ctrl 56.94 ± 3.75 (n = 5 mice; 67 villi)). Meanwhile, in the colon, no difference in crypt depth or width was found between the 60d-HFD and Ctrl groups (crypt depth, 60d-HFD group 70.57 ± 2.31 (n = 6 mice; 131 crypts) *vs* Ctrl 69.27 ± 4.73 (n = 6 mice; 131 crypts); crypt width, 60d-HFD group 29.54 ± 1.18 (n = 6 mice; 131 crypts) *vs* Ctrl 30.31 ± 1.21 (n = 6 mice; 131 crypts)). Taken all together, these results indicate a reduction in the surface area of the ileum of HFD-fed mice in comparison with the controls, corroborating the intestinal permeability data.

As part of the objectives of the present work, we went to investigate whether *in vitro* exposure to FFA, one of the main components of HFD, could affect the TJ-mediated epithelial barrier of Caco-2, a human colonic cell line frequently used as a model of intestinal epithelial barrier in general [42,43]. As shown in Table 1, no significant changes in R_T and F_T to the paracellular small-sized marker phenol red were observed across Caco-2 monolayers when exposed to different FFAs, namely the palmitic acid (PA), the oleic acid (OA), and the linoleic acid (LA), for 24 h at concentrations of 200 μM and 400 μM, in comparison with control monolayers. Treatment with the highest concentration tested

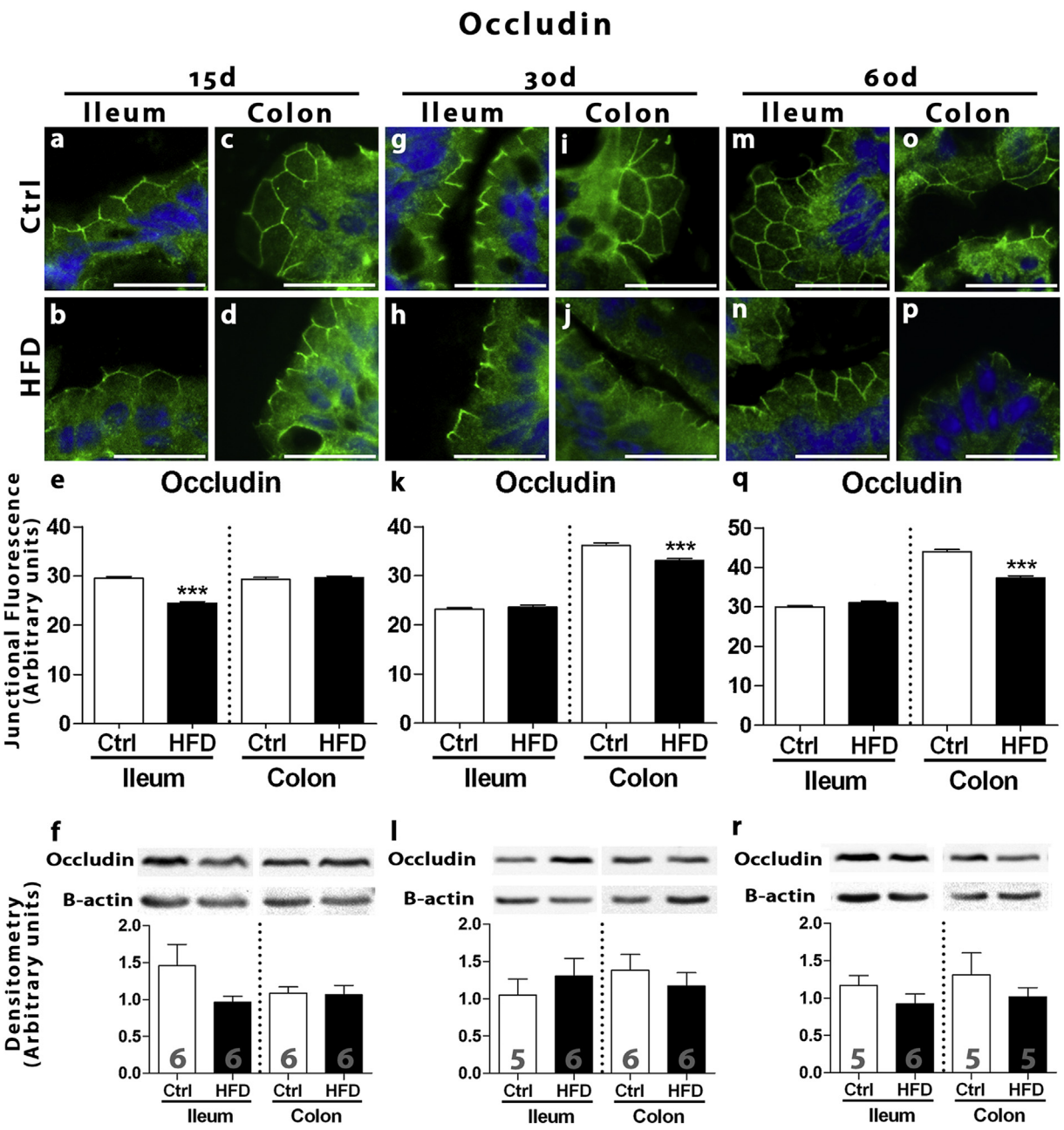

Fig. 6. Cellular distribution and content of Occludin in the epithelium of ileum and colon from mice fed a standard (Ctrl) or high-fat diet (HFD) for 15d, 30d and 60d. Images a-d, g-j, m-p show the junctional labeling of occludin evidenced by immunofluorescence (FITC in green, DAPI-blue labeling of the nucleus) in cryosections of ileum and colon of mice treated with HFD for different periods. The images of Ctrl and HFD groups are representative, obtained from the same immunofluorescence and microscopic session. HFD induced a significant decrease of occludin junctional content in the ileal epithelium after 15 d (e) and in the colon epithelium after 30 d (k) and 60 d of treatment (q) in comparison with the control group. The immunoblotting did not show significant changes in the total cell content of occludin in mice fed HFD during 15d (f), 30d (l) or 60d (r). Bar, 25 μm. The number inside the bars shows the number of animals for each group. The values represent the mean ± SEM. ***P < 0.0001 compared to its Ctrl group (Student t-test). (For interpretation of the references to colour in this figure legend, the reader is referred to the Web version of this article.)

(400 μM) of each FFA also did not altered the paracellular permeability to the FITC-dextran across the Caco-2 monolayers (Control 3.54 ± 0.45% (5); PA 3.52 ± 0.36% (5); OA 3.08 ± 0.32% (5); LA 3.71 ± 0.83% (5), percentage in relation to the sum of the absorbance of basal plus apical solutions (Abs_{a+b})(considered as 100% of the marker concentration)). Nevertheless, the immunofluorescence analysis of some TJ proteins revealed an increase of the junctional content of claudin-1 and ZO-1, but not of occludin, in monolayers when exposed to 400 μM of palmitic acid and 200 μM and 400 μM of linoleic acid (Fig. 8). However, western blotting showed no differences in the total cell content of these proteins after exposure to the two FFAs at both concentrations (Fig. 8). Meanwhile, the treatment with oleic acid resulted in a more diverse effect that included no significant changes in claudin-1 at both concentrations, a decrease in occludin associated with an increase in ZO-1 junctional contents at concentration of 200 μM but a decrease in junctional content of both proteins at the higher concentration (400 μM) (Fig. 8). Immunoblotting revealed significant change (a decrease) only in ZO-1 cell content after 400 μM oleic acid exposure (Fig. 8).

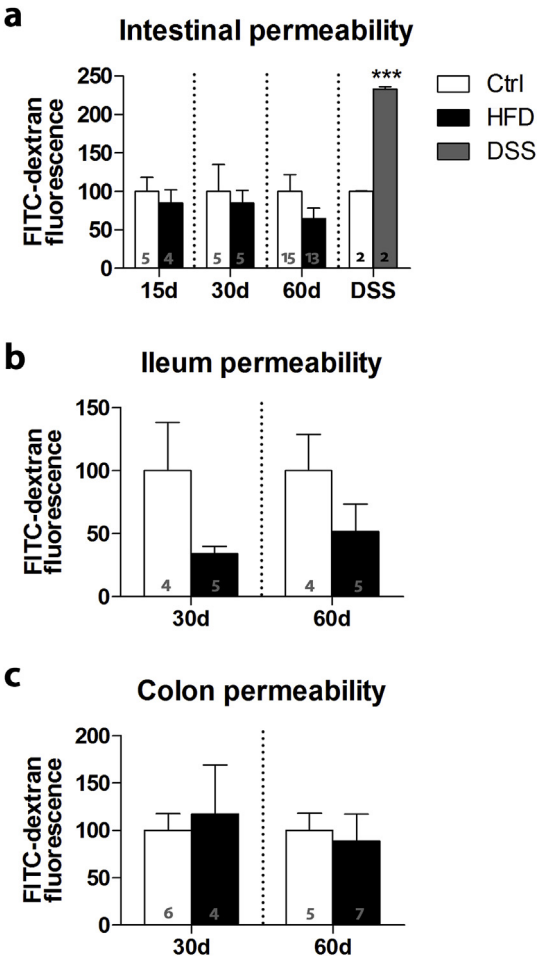

Fig. 7. Intestinal permeability in mice fed a standard (Ctrl) or high-fat diet (HFD) for 15d, 30d and 60d. The intestinal permeability was assessed using the paracellular FITC-dextran marker given to the animal by gavage (a) or injected within intestine sacs *in situ* (b, c). The graph in (a) shows no significant changes in mouse intestinal permeability after HFD intake up to 60d. Assessment of the paracellular permeability in isolated intestine segments also revealed no significant alteration in the ileum (b) and colon (c) permeabilities after 30d or 60d HFD treatment in relation to the control group. As a positive control, mice were treated with dextran sulfate sodium (DSS) to induce ulcerative colitis in order to evaluate the intestinal permeability test by gavage. Plasma levels of FITC-dextran were higher in animals treated with DSS, indicating a significant increase in intestinal permeability (a). Results are expressed as mean ± SEM of the percentage in relation to the Ctrl; n samples shown in the graph bar. ***P < 0.001 as compared to its Ctrl group (Student t-test).

4. Discussion

Clinical and experimental studies have suggested an association among high-fat diet intake (HFD), intestinal microbiota imbalance (dysbiosis), increased intestinal permeability and peripheral insulin resistance [10,11,29,33]. The ongoing hypothesis, that attempts to explain the involvement of the intestinal microbiota in the pathogenesis of diabetes, suggests that the change in composition of this microbiota, due to, in part, the high-fat low-fiber diet intake, is associated with an increased level of LPS in the blood, as a consequence of a rise in intestinal permeability, that results in endotoxemia which in turn triggers or aggravates the insulin resistance state [10,11,29]. Although this hypothesis of the dysbiosis - endotoxemia - insulin resistance axis is widespread and currently accepted [41,53,54], little is known about the TJ dynamics and intestinal paracellular barrier integrity during the T2DM evolution. In the present study, we investigated for the first time

Table 1
Transepithelial electrical resistance (R_T) and transepithelial flux (F_T) analysis in. Caco-2 monolayers exposed to palmitic, oleic, or linoleic acids.

Group	Parameter	
	R_T (% initial value)	$F_{T\ phenol\ red}$ (% Abs_{a+b})
Palmitic Acid		
Control	101.00 ± 5.56 (7)	16.83 ± 1.63 (11)
200 μM	92.00 ± 4.63 (7)	17.00 ± 1.25 (12)
400 μM	92.21 ± 4.74 (7)	18.63 ± 1.23 (12)
Oleic Acid		
Control	95.44 ± 4.03 (7)	18.39 ± 1.47 (9)
200 μM	98.18 ± 6.61 (7)	19.16 ± 2.11(9)
400 μM	92.59 ± 4.45 (7)	18.59 ± 1.46 (9)
Linoleic Acid		
Control	93.05 ± 2.32 (6)	18.40 ± 1.45 (9)
200 μM	92.88 ± 2.53 (6)	19.20 ± 2,79 (9)
400 μM	94.27 ± 2.27 (6)	15.62 ± 1.56 (9)

Monolayers were treated with FFA for 24 h at concentrations of 200 or 400 μM. For the measurement of the F_T, phenol red was used as a paracellular marker. Value ± SEM (number of monolayers); R_T data are expressed as percentage of initial R_T value; F_T data are expressed as percentage in relation to the sum of the absorbance of the basal plus the apical solution (Abs_{a+b}) (considered as 100% of the marker concentration) (One-way ANOVA followed by Bonferroni post-test; no significant difference).

a possible temporal correlation between the development of prediabetes induced by HFD in mice and the alteration of the intestinal epithelial barrier mediated by the TJ in the distal intestine, namely ileum and colon. The reason to focus on these two intestinal segments is that, since they concentrate most of the microbiota [16,40,41], they would be more affected by a dysbiosis as resulted of high-fat feeding.

Our experiments showed that HFD intake for two weeks is sufficient to induce weight gain and higher levels of postprandial glycemia and cholesterolemia. As the animals continued to consume HFD, weight gain and postprandial hyperglycemia enhanced, which was accompanied by an increase in the fasting glycemia and triglyceride plasma level at one month of treatment, and after two months, HFD induced also hyperinsulinemia and increased LDL plasma concentration, associated with peripheral insulin resistance. Thus, exposure to HFD induces progressive changes in carbohydrate and lipid metabolism in mice from 15d, which worsens until the development of a typical prediabetes state at 60d of treatment [5,36,55,56].

Regarding the intestinal epithelial barrier, we demonstrated that a subtle, in some cases transient, but significant TJ structural alterations can be detected in the intestinal epithelium of ileum and colon mainly when the prediabetes has been established in our model, induced by HFD ingestion for 60d. The junctional content of TJ proteins, assessed at the cell-to-cell contact by immunofluorescence, showed a decrease in Cld-1 (in the ileum and colon segments) and Cld-3 (ileum) and occludin (colon) in prediabetic mice. These junctional proteins are well known to interact with each other to form the TJ strands and regulate the epithelial barrier function to ions and molecules [57–59]. The analysis of Cld-2 (that regulates the paracellular permeability to cations/water [57,60]) showed a significant reduction in the total and junctional contents of this protein in the ileum, while an increase in its junctional content was seen in the colon of mice after 60d HFD exposure. However, the data on total cell level of these junctional proteins revealed by Western Blot did not accompany those observed by immunofluorescence (except for claudin-2 in the ileum). While immunofluorescence analysis represents the amount of proteins present at the TJ site, the immunoblotting analysis reflects the total concentration of these proteins within the cell, that includes both pools: that associated to the plasma membrane (at the cell-cell contact) and that dispersed in the cytoplasm [61,62].

The TJ impairment observed in this work probably represents relatively rapid and possibly reversible changes that involve events of

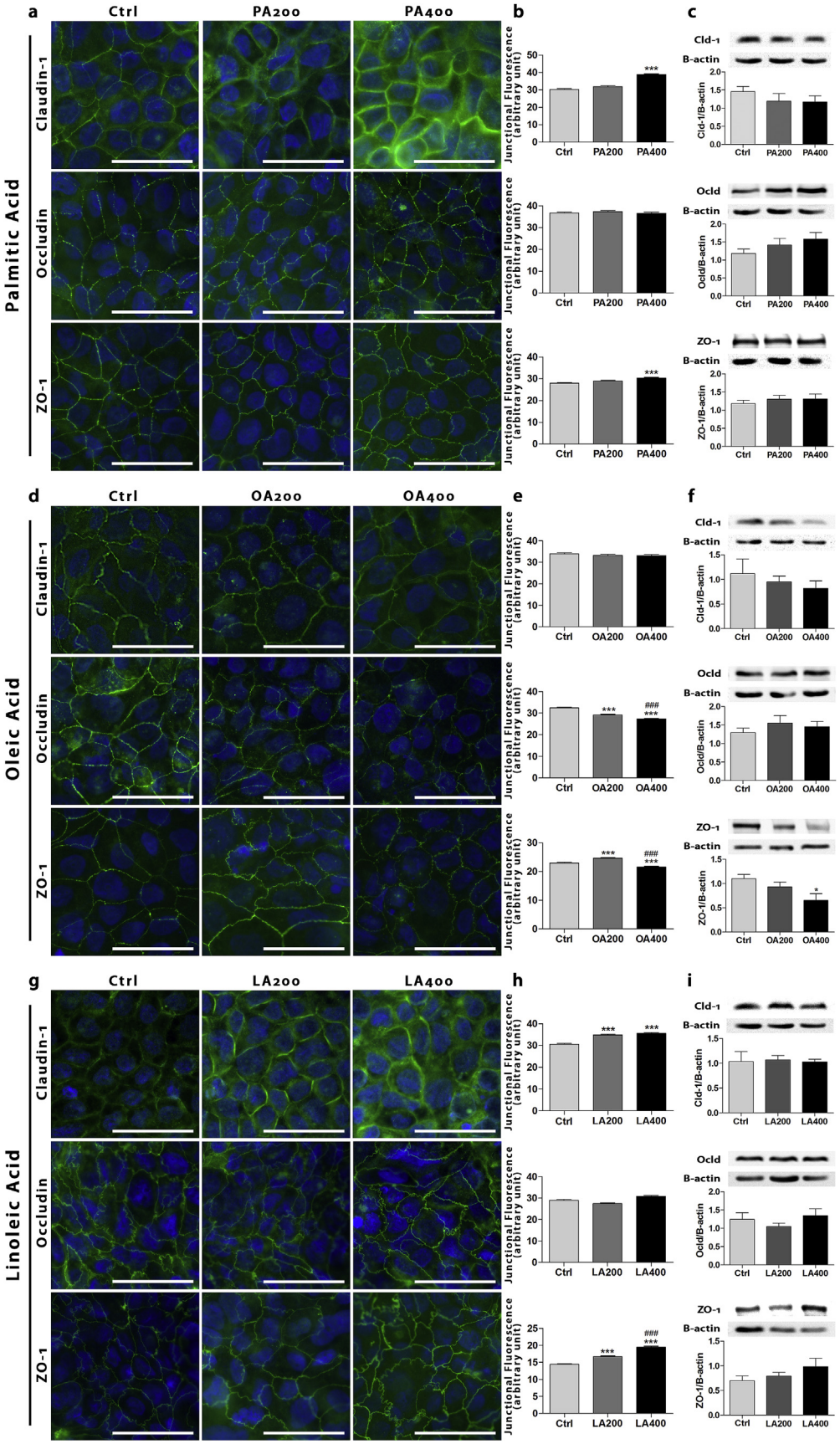

Fig. 8. Cellular distribution and content of tight junction (TJ) proteins in Caco-2 monolayers exposed to free fatty acids (palmitic, oleic and linoleic acid) for 24h. Images a, d and g show the immunofluorescence labeling of claudin-1, occludin, and ZO-1 in Caco-2 monolayers. Palmitic acid (400 μM, b) and linoleic acid (200 μM and 400 μM, h) induced a significant increase of claudin-1 and ZO-1, while treatment with oleic acid (200 μM and 400 μM, e) resulted in a decreased occludin junctional content but a concentration-dependent changes in ZO-1 at the cell-to-cell contact in relation to the control group (Ctrl) (n = 3–6 monolayers/group of 2–5 independent experiments). Immunoblotting analyses show no significant changes in the total cellular content of these TJ proteins after palmitic and linoleic acid treatments (c, i), but a significant decrease in ZO-1 cell content was observed after 400 μM oleic acid exposure (f) (n = 7–10 monolayers/group). Bar, 50 μm ***P < 0.0001 in relation to Ctrl group; ###P < 0.0001 compared to the 200 μM group (One-way ANOVA; Bonferroni post-test).

internalization of junctional proteins, as well as changes in the dynamics and interactions between these proteins at the TJ site, rather than alterations to gene/protein expression. Cell internalization/redistribution of claudins and occludin has been related to epithelial barrier disruption in several *in vitro* and *in vivo* conditions [63–68]. Although the intracellular mechanisms involved in assembly and disassembly of junctional proteins are not fully understood, several works have shown that the degree of phosphorylation/dephosphorylation of junctional proteins is crucial for the localization and stability of these proteins at the TJ region [25,57,69–71]. In addition, the removal of the junctional proteins from their membrane site may occur through other post-translational modifications such as palmitoylation and ubiquitination, which in turn may result in the transport of such proteins to the degradation pathway or recycle them to the membrane, hence modulating the TJ permeability and selectivity [25,61,64,66,72]. Therefore, it is plausible to suggest that the alteration to the TJ structure seen in the intestinal epithelia of prediabetic animals may involve one of these mechanisms of TJ regulation. Altogether, our results point to a subtle structural impairment of the TJ in the distal intestine of prediabetic mice, which is suggestive of increased intestinal permeability for small molecules and segment-dependent modulation of the paracellular sodium/water transport.

Surprisingly, the evaluation of intestinal permeability in our mice exposed to HFD, using the well known FITC-dextran marker, showed no significant difference in this parameter in relation to the Ctrl group in any studied periods. An additional assay to test a possible local intestinal permeability change, in which FITC-dextran was injected in isolated ileum and colon sacs, corroborated the *in vivo* experiment. In fact, we observed a tendency (but not statistically significant) of decrease in ileal permeability after 30d and 60d-HFD treatment that might be associated with the significant decrease in the absorption surface area of this segment as revealed by the morphometric analysis. Our data showing a lack of significant changes in intestinal permeability after HFD intake, however, differ from previously published data [10,34]. Cani et al. [10] have shown that a lipid-rich diet leads to increased intestinal permeability that correlates with decreased gene expression of the ZO-1 and occludin proteins. In an ex vivo system (Ussing Chamber), Stenman et al. [34] observed that HFD induces an increased permeability in the jejunum and colon epithelium but not in duodenum and ileum. In both studies, the duration of HFD treatment was only 30 d, however, the composition of such diets differ from the one used in our study (72% [10] and 60% [34] vs. 40% in energy content derived from lipids in ours). The higher intestinal permeability shown in these studies is probably due to more intense metabolic alterations, induced by those modified diets, that may be associated with a marked local inflammatory process and intestinal epithelial lesion, and therefore not directly related to the regulation of TJ [10,41,73].

In addition, at physiological conditions, TJ allows only the passage of molecules with a diameter smaller than 4 Å [23]; however, the probe employed herein and by other studies [10,33,34] to investigate the paracellular pathway is much larger (FITC-dextran 4 kDa has a diameter of 14 Å [74]). It has been suggested that the passage of these high molecular weight markers through normal epithelia is limited and represents small temporary breaks in the epithelial barrier [23]. Therefore, a higher concentration of these markers in plasma after administration by gavage, as observed herein after treatment with DSS or in other studies [10,34], reflects a substantial impairment of the intestinal epithelial barrier (probably with a considerable lesion of the intestinal epithelium itself). Our data showing that treatment with HFD containing 21% lipids results in a cellular redistribution of some TJ proteins in the ileal and colonic epithelia, without significant morphological changes in the intestinal epithelium or intestinal permeability to large molecules (such as FITC-dextran), are in agreement with this idea.

As an additional aim of this work, we investigated whether one of the components of the intestinal luminal environment, whose concentration may be potentially modified by the ingestion of HFD, could be involved in the changes of the epithelial barrier mediated by TJ observed here in the prediabetic animals and previously under *in vitro* conditions [31]. Free fatty acids (FFA), particularly the palmitic (PA), oleic (OA) and linoleic acids (LA), are some of those components whose concentration is significantly increased in obese and diabetic subjects plasma [50–52,75,76] and that are present in the lard and/or vegetable oil used as a source of lipids in our HFD [37–39]. Exposure of the Caco-2 cell line to these FFAs for 24 h, in concentrations compatible with those found in obese and diabetic individuals (200 and 400 μM) [51,75,76], was not associated with significant modifications in the R_T and neither in the paracellular flux to the phenol red and FITC-dextran, suggesting no significant alteration of the paracellular barrier function. Nevertheless, FFA treatment resulted in subtle, though statistically significant changes in the cellular distribution of TJ proteins in Caco-2 monolayers. Surprisingly, palmitic (AP) and linoleic (LA) acids appeared to strengthen the TJ structure since they induced an increase in the intercellular content of Cld-1 and ZO-1 in Caco-2 monolayers. Oleic acid (AO) treatment, in turn, had a diverse and dose-dependent effect, inducing a decrease in the junctional content of occludin at both concentrations tested and, for ZO-1, at the concentration of 200 μM, a slight increase in the amount of this protein in the intercellular region was observed whereas, at the concentration of 400 μM, the effect was the opposite. Such modifications in the localization of the TJ proteins induced by FFA exposure were not accompanied by changes in the total cellular content of these proteins, as assessed by Western Blot, except in the case of the 400 μM concentration of AO, which resulted in a significant decrease of ZO-1. Therefore, 24 h-treatment of an intestinal cell line with FFAs, given separately, could not reproduce the changes in intestinal TJ structure seen after HFD feeding, suggesting that these lipids may not be directly involved in the phenomenon. Nevertheless, an indirect effect of FFAs on the epithelial barrier via microbiota can not be discarded [13,14]. Further works focus on the effect of FFAs on microbiota composition and testing a more prolonged exposure of a combination of these FFAs, to better model the T2DM state, may shed light on this matter.

Studies investigating the *in vitro* effects of fatty acids on the integrity of the epithelial barrier present controversial results, although at high concentrations (on the millimolar scale) and/or chronic exposure, these FFA appear to significantly increase the paracellular permeability often associated with a cytotoxic effect [77–81]. These studies, evidencing the deleterious action of fatty acids on the epithelial barrier of different cell lines, are in contrast with our results. One possible explanation is the fact that these studies employed very high (pharmacological) concentrations of these agents (at least 12x higher than ours) while, in our work, FFA concentrations were used within the physiological range (50–750 μM [82]).

In conclusion, our work for the first time describes the evolution of metabolic disturbances in an animal model of type 2 prediabetes in parallel to the structure and function of TJ-mediated intestinal epithelial barrier of the distal intestinal segments, ileum and colon, chosen because they concentrate most of the intestinal microbiota [40,41]. We demonstrated that HFD induces progressive metabolic changes in mice leading to the development of fasting hyperglycemia associated with peripheral insulin resistance, hyperinsulinemia, and dyslipidemia, typical of the prediabetes state, after 60 days of treatment. Mainly after prediabetes has been established, subtle but statistically significant structural modifications of the TJ were observed in the epithelium of ileum and colon. These TJ alterations involved internalization/redistribution of junctional proteins, indicative of paracellular barrier disruption, but were not associated with a lesion of intestinal epithelium or increased intestinal permeability to large molecules. In addition, our *in vitro* study suggests that FFAs (i.e. palmitic, oleic and linoleic acids), that are enriched in HFD and increased in plasma of obese and diabetic patient [37,50,51,75,76], may not be accounted for the impaired TJ structure observed in our prediabetic mice and *in vitro* conditions after exposure to intestinal luminal content of these animals [31].

Altogether, our findings suggest that TJ-mediated intestinal epithelial barrier in the ileum and colon can be affected by HFD intake even at the early stage of T2DM, although the TJ changes in these intestinal segments were marginal and probably do not contribute to the disease onset. Yet, the involvement of the proximal intestinal, represented by duodenum and jejunum, can not be discarded [16]. It is possible that the progression of metabolic dysfunctions induced by more prolonged exposure to HFD may be accompanied by more severe changes in the epithelial barrier function mediated by the TJ, including other intestinal segments. This, in turn, would result in increased paracellular permeability of substances/molecules present in the intestinal lumen (i.e. LPS, food antigens, etc.), contributing to the low-grade systemic inflammatory state (typical of T2DM), with consequent worsening of peripheral resistance to insulin and the metabolic manifestations of T2DM.

Funding

This work was funded by grants from Fundação de Amparo à Pesquisa do Estado de São Paulo (FAPESP # 2013/15676-0 and 2018/02118-2, Brazil).

Declaration of Competing Interest

The authors declare that there are no conflicts of interest.

Acknowledgments

The authors thank Ms. Stephanie Souto Maior Federighi and Ms. Susely Ferraz de Siqueira Tada for the excellent technical assistance. The authors also thank Dr. Valéria H. A. C. Quitete, Dr. Elaine Minatel and Prof. Alexandre L. R. de Oliveira for allowing access to their laboratory facilities. CBC-B (CNPq# 308546/2018-0) is a recipient of Research Fellowship from Conselho Nacional de Desenvolvimento Científico e Tecnológico (CNPq, Brazil). RBO, VAM, and LCP were recipients of Ph.D. and MSc fellowships from CNPq (Brazil).

References

[1] A. Liston, J.A. Todd, V. Lagou, Beta-cell fragility as a common underlying risk factor in type 1 and type 2 diabetes, Trends Mol. Med. 23 (2017) 181–194, https://doi.org/10.1016/j.molmed.2016.12.005.

[2] D. Tripathy, A.O. Chavez, Defects in insulin secretion and action in the pathogenesis of type 2 diabetes mellitus, Curr. Diabetes Rep. 10 (2010) 184–191, https://doi.org/10.1007/s11892-010-0115-5.

[3] M. Prentki, C.J. Nolan, Islet β-cell failure in type 2 diabetes, J. Clin. Investig. 116 (2006) 1802–1812, https://doi.org/10.1172/JCI29103.1802.

[4] American Diabetes Association, Diagnosis and classification of diabetes mellitus, Diabetes Care 37 (2014) 81–90, https://doi.org/10.2337/dc14-S081.

[5] R.B. Oliveira, C.P.F. Carvalho, C.C. Polo, G.G. Dorighello, C. Boschero, H.C.F. Oliveira, C.B. Collares-Buzato, Impaired compensatory beta-cell function and growth in response to high-fat diet in LDL receptor knockout mice, Int. J. Exp. Pathol. 95 (2014) 296–308, https://doi.org/10.1111/iep.12084.

[6] C.J. Rhodes, Type 2 Diabetes - a matter of ß-cell life and death? Science 80 (2005) 380–383, https://doi.org/10.1126/science.1104345 307.

[7] C.B. Collares-Buzato, High-fat diets and β-cell dysfunction: molecular aspects, in: D. Mauricio (Ed.), Mol. Nutr. Diabetes, first ed., Elsevier, 2016, pp. 115–130.

[8] P. Arner, M. Rydén, Fatty acids , obesity and insulin resistance, Obes Facts 8 (2015) 147–155, https://doi.org/10.1159/000381224.

[9] J. Amar, C. Chabo, A. Waget, P. Klopp, C. Vachoux, L.G. Bermúdez-Humarán, N. Smirnova, M. Bergé, T. Sulpice, S. Lahtinen, A. Ouwehand, P. Langella, N. Rautonen, P.J. Sansonetti, R. Burcelin, Intestinal mucosal adherence and translocation of commensal bacteria at the early onset of type 2 diabetes: molecular mechanisms and probiotic treatment, EMBO Mol. Med. 3 (2011) 559–572, https://doi.org/10.1002/emmm.201100159.

[10] P.D. Cani, R. Bibiloni, C. Knauf, A.M. Neyrinck, N.M. Delzenne, Changes in gut microbiota control metabolic diet–induced obesity and diabetes in mice, Diabetes 57 (2008) 1470–1481, https://doi.org/10.2337/db07-1403.

[11] P.D. Cani, J. Amar, M.A. Iglesias, M. Poggi, C. Knauf, D. Bastelica, A.M. Neyrinck, F. Fava, K.M. Tuohy, C. Chabo, J. Ferrie, G.R. Gibson, L. Casteilla, N.M. Delzenne, M.C. Alessi, Metabolic endotoxemia initiates obesity and insulin resistance, Diabetes 56 (2007) 1761–1772, https://doi.org/10.2337/db06-1491.

[12] M. Balakumar, D. Prabhu, C. Sathishkumar, P. Prabu, Improvement in glucose tolerance and insulin sensitivity by probiotic strains of Indian gut origin in high - fat diet-fed C57BL/6J mice, Eur. J. Nutr. 57 (2018) 279–295, https://doi.org/10.1007/s00394-016-1317-7.

[13] S. De Kort, D. Keszthelyi, A.A.M. Masclee, Leaky gut and diabetes mellitus: what is the link? Obes. Rev. 12 (2011) 449–458, https://doi.org/10.1111/j.1467-789X.2010.00845.x.

[14] A. Everard, P.D. Cani, Diabetes, obesity and gut microbiota, Best Pract. Res. Clin. Gastroenterol. 27 (2013) 73–83, https://doi.org/10.1016/j.bpg.2013.03.007.

[15] S.S. Ghosh, J. Bie, J. Wang, S. Ghosh, Oral supplementation with non-absorbable antibiotics or curcumin attenuates western diet-induced atherosclerosis and glucose intolerance in LDLR -/- mice – role of intestinal permeability and macrophage activation, PLoS One 9 (2014), https://doi.org/10.1371/journal.pone.0108577 e108577.

[16] T.P.M. Scheithauer, G.M. Dallinga-Thie, W.M. De Vos, M. Nieuwdorp, D.H. Van Raalte, Causality of small and large intestinal microbiota in weight regulation and insulin resistance, Mol. Metab. 5 (2016) 759–770, https://doi.org/10.1016/j.molmet.2016.06.002.

[17] M. Spiljar, D. Merkler, M. Trajkovski, The immune system bridges the gut microbiota with systemic energy homeostasis: focus on TLRs, mucosal barrier, and SCFAs, Front. Immunol. 8 (2017) 1–10, https://doi.org/10.3389/fimmu.2017.01353.

[18] C.L. Bevins, N.H. Salzman, Paneth cells, antimicrobial peptides and maintenance of intestinal homeostasis, Nat. Rev. Microbiol. 9 (2011) 356–368, https://doi.org/10.1038/nrmicro2546.

[19] M.E.V. Johansson, H. Sjövall, G.C. Hansson, The gastrointestinal mucus system in health and disease, Nat. Rev. Gastroenterol. Hepatol. 10 (2013) 352–361, https://doi.org/10.1038/nrgastro.2013.35.

[20] J.M. Brandner, J.D. Schulzke, Hereditary barrier-related diseases involving the tight junction: lessons from skin and intestine, Cell Tissue Res. 360 (2015) 723–748, https://doi.org/10.1007/s00441-014-2096-1.

[21] M.M. France, J.R. Turner, The mucosal barrier at a glance, J. Cell Sci. 130 (2017) 307–314, https://doi.org/10.1242/jcs.193482.

[22] D. Günzel, Claudins: vital partners in transcellular and paracellular transport coupling, Pflugers Arch. Eur. J. Physiol. 469 (2017) 35–44, https://doi.org/10.1007/s00424-016-1909-3.

[23] J.M. Anderson, C.M. Van Itallie, Physiology and function of the tight junction, Cold Spring Harb. Perspect. Biol. 1 (2009) 1–16, https://doi.org/10.1101/cshperspect.a002584.

[24] S.F. Assimakopoulos, I. Papageorgiou, A. Charonis, Enterocytes' tight junctions: from molecules to diseases, World J. Gastrointest. Pathophysiol. 6 (2011) 123–137, https://doi.org/10.4291/wjgp.v2.i6.123.

[25] D. Gunzel, A.S.L. Yu, Claudins and the modulation of tight junction permeability, Physiol. Rev. 93 (2013) 525–569, https://doi.org/10.1152/physrev.00019.2012.

[26] K. Ebnet, Organization of multiprotein complexes at cell-cell junctions, Histochem. Cell Biol. 130 (2008) 1–20, https://doi.org/10.1007/s00418-008-0418-7.

[27] A. Fasano, Physiological, pathological, and therapeutic implications of Zonulin-mediated intestinal barrier modulation, Am. J. Pathol. 173 (2008) 1243–1252, https://doi.org/10.2353/ajpath.2008.080192.

[28] P.A. Bron, M. Kleerebezem, R. Brummer, P.D. Cani, A. Mercenier, T.T. Macdonald, C.L. Garcia-Ródenas, J.M. Wells, Can probiotics modulate human disease by impacting intestinal barrier function ? Br. J. Nutr. 117 (2017) 93–107, https://doi.org/10.1017/S0007114516004037.

[29] A. Sabatino, G. Regolisti, C. Cosola, L. Gesualdo, E. Fiaccadori, Intestinal microbiota in type 2 diabetes and chronic kidney disease, Curr. Diabetes Rep. 17 (2017), https://doi.org/10.1007/s11892-017-0841-z.

[30] V. Matheus, L. Monteiro, R. Oliveira, D. Maschio, C.B. Collares-Buzato, Butyrate reduces high-fat diet-induced metabolic alterations, hepatic steatosis and pancreatic beta cell and intestinal barrier dysfunctions in prediabetic mice, Exp. Biol. Med. (2017), https://doi.org/10.1177/1535370217708188 153537021770818.

[31] R.B. Oliveira, L.P. Canuto, C.B. Collares-Buzato, Intestinal luminal content from high-fat-fed prediabetic mice changes epithelial barrier function in vitro, Life Sci. 216 (2019) 10–21, https://doi.org/10.1016/j.lfs.2018.11.012.

[32] M. Secondulfo, D. Iafusco, R. Carratù, L. deMagistris, A. Sapone, M. Generoso, A. Mezzogiorno, F.C. Sasso, M. Cartenì, R. De Rosa, F. Prisco, V. Esposito, Ultrastructural mucosal alterations and increased intestinal permeability in non-celiac, type I diabetic patients, Dig. Liver Dis. 36 (2004) 35–45, https://doi.org/10.1016/j.dld.2003.09.016.

[33] C.B. La Serre, C.L. Ellis, J. Lee, A.L. Hartman, J.C. Rutledge, H.E. Raybould, Propensity to high-fat diet-induced obesity in rats is associated with changes in the gut microbiota and gut inflammation, Am. J. Physiol. Gastrointest. Liver Physiol. 299 (2010) 440–448, https://doi.org/10.1152/ajpgi.00098.2010.

[34] L.K. Stenman, R. Holma, R. Korpela, High-fat-induced intestinal permeability dysfunction associated with altered fecal bile acids, World J. Gastroenterol. 18 (2012) 923–929, https://doi.org/10.3748/wjg.v18.i9.923.

[35] D. Zhang, L. Zhang, Y. Zheng, F. Yue, R.D. Russell, Y. Zeng, Circulating zonulin levels in newly diagnosed Chinese type 2 diabetes patients, Diabetes Res. Clin. Pract. 106 (2014) 312–318, https://doi.org/10.1016/j.diabres.2014.08.017.

[36] R.B. Oliveira, D.A. Maschio, C.P.F. Carvalho, C.B. Collares-Buzato, Influence of gender and time diet exposure on endocrine pancreas remodeling in response to high fat diet-induced metabolic disturbances in mice, Ann. Anat. 200 (2015) 88–97, https://doi.org/10.1016/j.aanat.2015.01.007.

[37] R.C. Silva, L.N. Cotting, T.P. Poltronieri, V.M. Balcão, L.A. Gioielli, Physical properties of structured lipids from lard and soybean oil produced by enzymatic interesterification, Cienc. Tecnol. Aliment. 29 (2009) 652–660.

[38] A. Rohman, K. Triyana, Sismindari, Y. Erwanto, Differentiation of lard and other animal fats based on triacylglycerols composition and principal component analysis, Int. Food Res. J. 19 (2012) 475–479.

[39] N.N.A. Nizar, J.M.N. Marikkar, D.M. Hashim, Differentiation of lard , chicken fat ,

beef fat and mutton fat by GCMS and EA-IRMS techniques, J. Oleo Sci. 62 (2013) 459–464.
[40] R. Sender, S. Fuchs, R. Milo, Revised estimates for the number of human and bacteria cells in the body, PLoS Biol. (2016) 1–14, https://doi.org/10.1371/journal.pbio.1002533.
[41] L. Wen, A. Duffy, Factors influencing the gut microbiota, inflammation, and type 2 diabetes, J. Nutr. (2017) 1468S–1472S, https://doi.org/10.3945/jn.116.240754.
[42] Y. Sambuy, I. De Angelis, G. Ranaldi, M.L. Scarino, A. Stammati, F. Zucco, The Caco-2 cell line as a model of the intestinal barrier: influence of cell and culture-related factors on Caco-2 cell functional characteristics, Cell Biol. Toxicol. 21 (2005) 1–26, https://doi.org/10.1007/s10565-005-0085-6.
[43] F. Zucco, A. Batto, G. Bises, J. Chambaz, A. Chiusolo, R. Consalvo, H. Cross, G. Dal Negro, I. de Angelis, G. Fabre, F. Guillou, S. Hoffman, L. Laplanche, E. Morel, M. Pinçon-Raymond, P. Prieto, L. Turco, G. Ranaldi, M. Rousset, Y. Sambuy, M. Scarino, F. Torreilles, A. Stammati, An inter-laboratory study to evaluate the effects of medium composition on the differentiation and barrier function of Caco-2 cell lines, Altern Lab Anim 33 (2005) 603–618.
[44] B. Abbas, T.L. Hayes, D.J. Wilson, K.E. Carr, Internal structure of the intestinal villus: morphological and morphometric observations at different levels of the mouse villus, J. Anat. 162 (1989) 263–273.
[45] Y.L. Ng, B. Klopcic, F. Lloyd, C. Forrest, W. Greene, I.C. Lawrance, Secreted protein acidic and rich in cysteine (SPARC) exacerbates colonic inflammatory symptoms in Dextran Sodium Sulphate-induced murine colitis, PLoS One 8 (2013) 2–9, https://doi.org/10.1371/journal.pone.0077575.
[46] M. Zayat, L.M. Lichtenberger, E.J. Dial, Pathophysiology of LPS-induced gastrointestinal injury in the rat, Shock 30 (2007) 206–211, https://doi.org/10.1097/shk.0b013e318160f47f.
[47] S.D. Hauschka, I.R. Konigsberg, The influence of collagen on the development of muscle clones, Proc. Natl. Acad. Sci. U.S.A. 55 (1966) 119–126, https://doi.org/10.1073/pnas.55.1.119.
[48] F. Allagnat, F. Alonso, D. Martin, A. Abderrahmani, G. Waeber, J.A. Haefliger, ICER-1γ overexpression drives palmitate-mediated connexin36 down-regulation in insulin-secreting cells, J. Biol. Chem. 283 (2008) 5226–5234, https://doi.org/10.1074/jbc.M708181200.
[49] J.L. Nano, C. Nobili, F. Girard-Pipau, P. Rampal, Effects of fatty acids on the growth of Caco-2 cells, Prostaglandins Leukot, Essent. Fat. Acids. 69 (2003) 207–215, https://doi.org/10.1016/S0952-3278(03)00083-8.
[50] Y. Ni, L. Zhao, H. Yu, X. Ma, Y. Bao, C. Rajani, L.W.M. Loo, Y.B. Shvetsov, H. Yu, T. Chen, Y. Zhang, C. Wang, C. Hu, M. Su, G. Xie, A. Zhao, W. Jia, W. Jia, Circulating unsaturated fatty acids delineate the metabolic status of obese individuals, EBioMedicine 2 (2015) 1513–1522, https://doi.org/10.1016/j.ebiom.2015.09.004.
[51] J.Y. Kim, J.Y. Park, O.Y. Kim, B.M. Ham, H.-J. Kim, D.Y. Kwon, Y. Jang, J.H. Lee, Metabolic profiling of plasma in overweight/obese and lean men using ultra performance liquid chromatography and Q-TOF mass spectrometry (UPLC− Q-TOF MS), J. Proteome Res. 9 (2010) 4368–4375, https://doi.org/10.1021/pr100101p.
[52] V.P. Dole, A relation between non-esterified fatty acids in plasma and the metabolism of glucose, J. Clin. Investig. 35 (1956) 350–357, https://doi.org/10.1172/JCI103259.
[53] Y.S.A. Moya-Pérez, Microbiota, inflammation and obesity, in: M. Lyte, J.F. Cryan (Eds.), Microbial Endocrinology: Microbiota-Gut-Brain Axis in Health and Diseases, Advances in Experimental Medicine and Biology 817, Springer, New York, 2014, pp. 291–317, , https://doi.org/10.1007/978-1-4939-0897-4.
[54] Z. Gao, Q. Li, X. Wu, X. Zhao, L. Zhao, X. Tong, New insights into the mechanisms of Chinese herbal products on diabetes : a focus on the " Bacteria-Mucosal Immunity-Inflammation-Diabetes " Axis, J. Immunol. Res. 2017 (2017) 1–13, https://doi.org/10.1155/2017/1813086.
[55] C.P.F. Carvalho, R.B. Oliveira, A. Britan, J.C. Santos-Silva, A.C. Boschero, P. Meda, C.B. Collares-Buzato, Impaired β-cell-β-cell coupling mediated by Cx36 gap junctions in prediabetic mice, Am. J. Physiol. Endocrinol. Metab. 303 (2012) E144–E151, https://doi.org/10.1152/ajpendo.00489.2011.
[56] D.A. Maschio, R.B. Oliveira, M.R. Santos, C.P.F. Carvalho, H.C.L. Barbosa-Sampaio, C.B. Collares-Buzato, Activation of the Wnt/β-catenin pathway in pancreatic beta cells during the compensatory islet hyperplasia in prediabetic mice, Biochem. Biophys. Res. Commun. 478 (2016) 1534–1540, https://doi.org/10.1016/j.bbrc.2016.08.146.
[57] L. Shen, C.R. Weber, D.R. Raleigh, D. Yu, J.R. Turner, Tight junction pore and leak pathways: a dynamic duo, Annu. Rev. Physiol. 73 (2011) 283–309, https://doi.org/10.1146/annurev-physiol-012110-142150.
[58] L. Shen, Tight junctions on the move: molecular mechanisms for epithelial barrier regulation, Ann. N. Y. Acad. Sci. 1258 (2012) 9–18, https://doi.org/10.1111/j.1749-6632.2012.06613.x.
[59] A. Lingaraju, T.M. Long, Y. Wang, J.R. Austin, J.R. Turner, Conceptual barriers to understanding physical barriers, Semin. Cell Dev. Biol. 42 (2015) 13–21, https://doi.org/10.1016/j.semcdb.2015.04.008.
[60] R. Rosenthal, S. Milatz, S.M. Krug, B. Oelrich, J.-D. Schulzke, S. Amasheh, D. Gunzel, M. Fromm, Claudin-2, a component of the tight junction, forms a paracellular water channel, J. Cell Sci. 123 (2010) 1913–1921, https://doi.org/10.1242/jcs.060665.
[61] J.D. Dukes, L. Fish, J.D. Richardson, E. Blaikley, S. Burns, C.J. Caunt, A.D. Chalmers, P. Whitley, Functional ESCRT machinery is required for constitutive recycling of claudin-1 and maintenance of polarity in vertebrate epithelial cells, Mol. Biol. Cell 22 (2011) 3192–3205, https://doi.org/10.1091/mbc.E11-04-0343.
[62] C.B. Collares-Buzato, C.P.F. Carvalho, A.G. Furtado, A.C. Boschero, Upregulation of the expression of tight and adherens junction-associated proteins during maturation of neonatal pancreatic islets in vitro, J. Mol. Histol. 35 (2004) 811–822, https://doi.org/10.1007/s10735-004-1746-0.
[63] M. Utech, R. Mennigen, M. Bruewer, Endocytosis and recycling of tight junction proteins in inflammation, J. Biomed. Biotechnol. 2010 (2010), https://doi.org/10.1155/2010/484987.
[64] A.D. Chalmers, P. Whitley, Continuous endocytic recycling of tight junction proteins: how and why? Essays Biochem. 53 (2012) 41–54, https://doi.org/10.1042/bse0530041.
[65] E.B.M.I. Peixoto, C.B. Collares-Buzato, Protamine-induced epithelial barrier disruption involves rearrangement of cytoskeleton and decreased tight junction-associated protein expression in cultured MDCK strains, Cell Struct. Funct. 29 (2005) 165–178, https://doi.org/10.1247/csf.29.165.
[66] L. Shen, C.R. Weber, J.R. Turner, The tight junction protein complex undergoes rapid and continuous molecular remodeling at steady state, J. Cell Biol. 181 (2008) 683–695, https://doi.org/10.1083/jcb.200711165.
[67] M. Furuse, K. Furuse, H. Sasaki, S. Tsukita, Conversion of zonulae occludentes from tight to leaky strand type by introducing claudin-2 into Madin-Darby canine kidney I cells, J. Cell Biol. 153 (2001) 263–272, https://doi.org/10.1083/jcb.153.2.263.
[68] B.M. Mongelli-Sabino, L.P. Canuto, C.B. Collares-Buzato, Acute and chronic exposure to high levels of glucose modulates tight junction-associated epithelial barrier function in a renal tubular cell line, Life Sci. 188 (2017) 149–157, https://doi.org/10.1016/j.lfs.2017.09.004.
[69] D.F. McCole, Phosphatase regulation of intercellular junctions, Tissue Barriers 2 (2013) e26713, , https://doi.org/10.4161/tisb.26713.
[70] D.R. Raleigh, D.M. Boe, D. Yu, C.R. Weber, A.M. Marchiando, E.M. Bradford, Y. Wang, L. Wu, E.E. Schneeberger, L. Shen, J.R. Turner, Occludin S408 phosphorylation regulates tight junction protein interactions and barrier function, J. Cell Biol. 193 (2011) 565–582, https://doi.org/10.1083/jcb.201010065.
[71] C.B. Collares-Buzato, M.A. Jepson, N.L. Simmons, B.H. Hirst, Increased tyrosine phosphorylation causes redistribution of adherens junction and tight junction proteins and perturbs paracellular barrier function in MDCK epithelia, Eur. J. Cell Biol. 76 (1998) 85–92, https://doi.org/10.1016/S0171-9335(98)80020-4.
[72] S. Takahashi, N. Iwamoto, H. Sasaki, M. Ohashi, Y. Oda, S. Tsukita, M. Furuse, The E3 ubiquitin ligase LNX1p80 promotes the removal of claudins from tight junctions in MDCK cells, J. Cell Sci. 122 (2009) 985–994, https://doi.org/10.1242/jcs.040055.
[73] H. Zhong, Y. Yuan, W. Xie, M. Chen, X. He, Type 2 diabetes mellitus Is associated with more serious small intestinal mucosal injuries, PLoS One 11 (2016), https://doi.org/10.1371/journal.pone.0162354 e0162354.
[74] L. Shi, M. Zeng, Y. Sun, B.M. Fu, Quantification of blood-brain barrier solute permeability and brain transport by multiphoton microscopy, J. Biomech. Eng. 136 (2014) 1–9, https://doi.org/10.1115/1.4025892.
[75] J.S. Pankow, B.B. Duncan, M.I. Schmidt, C.M. Ballantyne, D.J. Couper, R.C. Hoogeveen, S.H. Golden, Fasting plasma free fatty acids and risk of type 2 diabetes: the Atherosclerosis Risk in Communities study, Diabetes Care 27 (2004) 77–82, https://doi.org/10.2337/diacare.27.1.77.
[76] L. Wang, A.R. Folsom, Z.-J. Zheng, J.S. Pankow, J.H. Eckfeldt, Plasma fatty acid composition and incidence of diabetes in middle-aged adults: the Atherosclerosis Risk in Communities (ARIC) study, Am. J. Clin. Nutr. 78 (2003) 91–98, https://doi.org/10.1016/S0939-4753(03)80029-7.
[77] B. Aspenström-Fagerlund, L. Ring, P. Aspenström, J. Tallkvist, N.G. Ilbäck, A.W. Glynn, Oleic acid and docosahexaenoic acid cause an increase in the paracellular absorption of hydrophilic compounds in an experimental model of human absorptive enterocytes, Toxicology 237 (2007) 12–23, https://doi.org/10.1016/j.tox.2007.04.014.
[78] D. Pabla, F. Akhlaghi, H. Zia, Intestinal permeability enhancement of levothyroxine sodium by straight chain fatty acids studied in MDCK epithelial cell line, Eur. J. Pharm. Sci. 40 (2010) 466–472, https://doi.org/10.1016/j.ejps.2010.05.002.
[79] P.A. Bateman, K.G. Jackson, V. Maitin, P. Yaqoob, C.M. Williams, Differences in cell morphology, lipid and apo B secretory capacity in Caco-2 cells following long term treatment with saturated and monounsaturated fatty acids, Biochim. Biophys. Acta Mol. Cell Biol. Lipids 1771 (2007) 475–485, https://doi.org/10.1016/j.bbalip.2007.02.001.
[80] N.G. Ilbäck, M. Nyblom, J. Carlfors, B. Fagerlund-Aspenström, S. Tavelin, A.W. Glynn, Do surface-active lipids in food increase the intestinal permeability to toxic substances and allergenic agents? Med. Hypotheses 63 (2004) 724–730, https://doi.org/10.1016/j.mehy.2003.10.037.
[81] E.F. Murphy, C. Jewell, G.J. Hooiveld, M. Muller, K.D. Cashman, Conjugated linoleic acid enhances transepithelial calcium transport in human intestinal-like Caco-2 cells: an insight into molecular changes, Prostaglandins Leukot. Essent. Fatty Acids 74 (2006) 295–301, https://doi.org/10.1016/j.plefa.2006.03.003.
[82] M.J. Watt, A.J. Hoy, D.M. Muoio, R.A. Coleman, Distinct roles of specific fatty acids in cellular processes: implications for interpreting and reporting experiments, Am. J. Physiol. Metab. 302 (2012) E1–E3, https://doi.org/10.1152/ajpendo.00418.2011.